Inorganic Chemistry
Article

Inorg. Chem. **2009**, *48*, 10519–10527 **10519**
DOI: 10.1021/ic901861c

Facile Route to Nitrides: Transformation from Single Element to Binary and Ternary Nitrides at Moderate Temperature through a New Modified Solid-State Metathesis

Bo Song,*,†,‡,§ Xiaolong Chen,§ Jiecai Han,⊥ Jikang Jian,∥ Wanyan Wang,§ Hongbo Zuo,⊥ Xinghong Zhang,⊥ and Songhe Meng⊥

†*The Research Station on Material Science and Engineering for Postdoctoral Fellows,* ‡*Academy of Fundamental and Interdisciplinary Sciences,* ⊥*Center for Composite Materials, Harbin Institute of Technology, Harbin 150080, China,* §*Beijing National Laboratory for Condensed Matter Physics, Institute of Physics, Chinese Academy of Sciences, P.O.Box 603, Beijing 100190, China, and* ∥*Department o Physics, Xinjiang University, Urumchi,830046, China*

Received April 23, 2009

In this article, we report a new modified solid-state metathesis pathway to synthesize nitrides using Li_3N as a nitrification reagent to transform single element to nitrides. In this process, not only binary (including mono- and multinitrides) but also ternary nitrides can be approached by varying the molar ratio of Li_3N to a single element. A possible two-step reaction mechanism for Li_3N and single elements was proposed. This study provides a promising route to meet the increasing demand in energy savings and environmental protection for materials synthesis.

I. Introduction

As an important class of functional materials, metal nitrides have received increasing attention due to their superior chemical and physical properties.[1,2] These outstanding properties facilitate the industrial application of nitrides to many fields. Examples include refractory ceramics (AlN, TaN, TiN),[3,4] superhard materials (IrN_2, OsN_2),[5−14] catalysts (VN),[15] spintronics devices (GdN),[16] wear-resistant coatings [TiN, ZrN, CrN, (Ti,Al)N, Zr_3N_4],[17−19] semiconductor devices for optoelectronics (GaN, InN),[20−23] and so on. It is therefore of interest to explore a general route to approach most of the nitrides. In the past several decades, great efforts have been devoted to synthesize nitrides, and the available routes contain a wide range of synthesis techniques, such as nitridation of metal or metal oxides,[24,25]

*To whom correspondence should be addressed. E-mail: songbo@hit.edu.cn.

(1) Li, J. W.; Watanabe, T.; Sakamoto, N.; Wada, H.; Setoyama, T.; Yoshimura, M. *Chem. Mater.* **2008**, *20*, 2095.
(2) Li, J. W.; Watanabe, T.; Wada, H.; Setoyama, T.; Yoshimura, M. *Chem. Mater.* **2007**, *19*, 3592.
(3) Dahotre, N. B.; Kadolkar, P.; Shah, S. *Surf. Interface Anal.* **2001**, *31*, 659.
(4) Schlesser, R.; Dalmau, R.; Zhuang, D.; Collazo, R.; Sitar, Z. *J. Cryst. Growth* **2005**, *281*, 75.
(5) Jonathan, C. C.; Alexander, F. G.; Babak, S.; Cheryl, L. E.; Peter, G. M.; James, L. F.; Nelsonl, A. J. *Science* **2006**, *311*, 1275.
(6) Yu, R.; Zhan, Q.; Lutgard, C. D. J. *Angew. Chem., Int. Ed.* **2007**, *46*, 1136.
(7) Yu, R.; Zhang, X. F. *Appl. Phys. Lett.* **2005**, *86*, 121913.
(8) Yu, R.; Zhang, X. F. *Phys. Rev. B* **2005**, *72*, 054103.
(9) Yu, R.; Zhan, Q.; Zhang, X. F. *Appl. Phys. Lett.* **2006**, *88*, 051913.
(10) Young, A. F.; Sanloup, C.; Gregoryanz, E.; Scandolo, S.; Hemley, R. J.; Mao, H. K. *Phys. Rev. Lett.* **2006**, *96*, 155501.
(11) Gregoryanz, E.; Sanloup, C.; Somayazulu, M.; Badro, J.; Fiquet, G.; Mao, H. K.; Hemley, R. J. *Nat. Mater.* **2004**, *3*, 294.
(12) Patil, S. K. R.; Khare, S. V.; Tuttle, B. R.; Bording, J. K.; Kodambaka, S. *Phys. Rev. B* **2006**, *73*, 104118.
(13) Young, A. F.; Montoya, J. A.; Sanloup, C.; Lazzeri, M.; Gregoryanz, E.; Scandolo, S. *Phys. Rev. B* **2006**, *73*, 153102.
(14) von Appen, J.; Lumey, M.; Dronskowski, R. *Angew. Chem., Int. Ed.* **2006**, *45*, 4365.
(15) Rodriguez, P.; Brito, J.; Albornoz, A.; Labadi, M.; Pfaff, C.; Marrero, S.; Moronta, D.; Betancourt, P. *Catal. Commun.* **2004**, *5*, 79.
(16) Duan, C. G.; Sabiryanov, R. F.; Liu, J. J.; Mei, W. N.; Dowben, P. A.; Hardy, J. R. *Phys. Rev. Lett.* **2005**, *94*, 237201.
(17) Lei, M.; Zhao, H. Z.; Yang, H.; Li, P. G.; Tang, H. L.; Song, B.; Tang, W. H. *Diamond Relat. Mater.* **2007**, *16*, 1974.
(18) Lei, M.; Zhao, H. Z.; Yang, H.; Song, B.; Cao, L. Z.; Li, P. G.; Tang, W. H. *J. Alloys Compd.* **2008**, *460*, 130.
(19) Zerr, A.; Riedel, R.; Sekine, T.; Lowther, J. E.; Ching, W. Y.; Tanaka, I. *Adv. Mater.* **2006**, *18*, 2933.
(20) PalDey, S.; Deevi, S. C. *Mater. Sci. Eng., B* **2003**, *361*, 1.
(21) Chen, X. L.; Li, J. Y.; Cao, Y. G.; Lan, Y. C.; Li, H.; He, M.; Wang, C. Y.; Zhang, Z.; Qiao, Z. Y. *Adv. Mater.* **2000**, *19*, 1432.
(22) Song, B.; Jian, J. K.; Wang, G.; Zhang, Z. H.; Lei, M.; Bao, H. Q.; Chen, X. L. *Physica E* **2008**, *40*, 579.
(23) Song, B.; Jian, J. K.; Wang, G.; Bao, H. Q.; Chen, X. L. *J. Appl. Phys.* **2007**, *101*, 124302.
(24) Claridge, J. B.; York, A. P. E.; Brungs, A. J.; Green, M. L. H. *Chem. Mater.* **2000**, *12*, 132.
(25) Balkas, C. M.; Davis, R. F. *J. Am. Ceram. Soc.* **1996**, *79*, 2309.

Published on Web 10/19/2009

solvothermal routes,[26−39] carbothermal reduction,[40,41] laser deposition,[42−44] high pressure,[45] gas phase/solid-state precursor decomposition,[46−49] etc. However, a facile route to metal nitrides in large scale is still a challenge and should be developed to meet the increasing demand of nitrides from a variety of application fields. Up to now, only certain kinds of nitrides can be obtained by heating metals or oxides in flowing nitrogen at high temperatures since it is very difficult to break the N≡N triple bond. Incomplete conversions of precursors or decompositions of nitrides are often encountered in the conventional route in which ammonia was selected as the nitrogen source. Recently, Zhao et al.[50] reported a carbothermal reduction route to prepare GaN and VN, assisted by using g-C_3N_4 as nitrifying reagent, and then, Fischer et al.[51] utilized mesoporous g-C_3N_4 as sacrificial template to synthesize metal nitride nanoparticles. More recently, Buha et al. reported a transformation process from oxides to nitrides using cyanamide and urea as the nitrogen source.[52] These synthesis processes are often required to be performed at high temperature with the assistance of pungent NH_3 or other organic precursors. In addition, the remnant amorphous carbon as an impurity is detrimental to the properties of the obtained nitrides.

In the 1990s, Kaner et al.[53,54] and Parkin et al.[55,56] had independently developed a solid-state metathesis (SSM) route, respectively. This pathway has been proven to be effective in the synthesis of many compounds including sulfides, carbides, nitrides, etc.[57−65] The key to the so-called SSM route is exhibited in two features: (1) selection of proper precursor to form thermodynamically favored byproduct salts, such as LiCl, LiBr, or LiI; (2) sufficient heat released at the initial step drives the reaction to sustain itself to completion within a few seconds. However, the precursors of metal halides are hygroscopic and very expensive, incurring a handicap in the manipulations process and additional costs, which means that the SSM routes are not suitable to synthesize nitrides on a large scale. In an earlier paper, we reported a modified solid-state metathesis (MSSM) route to approach metal nitrides by using Li_3N as the nitrogen source and metal oxides as precursors.[66] In MSSM route, Li_3N exhibits a surprisingly nitrification ability to transform thermodynamically stable oxides such as α-Al_2O_3, TiO_2, ZrO_2, etc. to the corresponding nitrides. However, the nitrides from the MSSM route often suffered from the residual oxygen element which has a significant influence on their performance. In order to avoid the disturbance of the oxygen from the source, using a metal or nonmetal single substance rather than oxides as the precursor is a better selection to synthesize the nitrides.

In this article, we report a facile transformation from a metal or nonmetal simple substance to nitrides directly. Aluminum (Al), manganese (Mn), chromium (Cr), molybdenum (Mo), niobium (Nb), the nonmetals boron (B) and silicon (Si) powder, etc. were used as the precursor materials, and Li_3N was selected as the nitrifying reagent. The desired nitrides can be obtained upon heating the corresponding metal element with Li_3N together in a sealed stainless steel crucible at 700−850 °C under a nitrogen gas atmosphere. This route is a slow, moderate, unexplosive pathway and can be considered as a new MSSM process in which some new characteristics are involved: the products are strongly dependent on the molar ratio of Li_3N to precursors, that is, not only binary nitrides (such as BN, AlN, Si_3N_4, Cr_2N) but also ternary nitrides (such as Li_2SiN_2, Li_3AlN_2, Li_3BN_2, Li_9CrN_5, Li_7MnN_4, etc.) can still be approached by varying the molar ratio of Li_3N to metal or nonmetal single element, suggesting the great potential of this route as a general route to approach nitrides. The obtained products were characterized in a detailed manner, and a possible reaction mechanism for the reaction between Li_3N and a single element was proposed and discussed.

II. Experimental Section

Materials. Li_3N was homemade in the laboratory without further purification. Boron powder (99.4%, crystalline) was purchased from STERM CHEMICALS. Al powder (99.99%), Cr powder (99.9%), Si powders (99.9%), and Mo (99.99%) were

(26) Hu, J. Q.; Deng, B.; Zhang, W. X.; Tang, K. B.; Qian, Y. T. *Chem. Phys. Lett*. **2002**, *351*, 229.
(27) Qian, Y. T. *Adv. Mater*. **1999**, *11*, 1101.
(28) Xie, Y.; Qian, Y. T.; Wang, W. Z.; Zhang, S. Y.; Zhang, Y. H. *Science* **1996**, *272*, 1926.
(29) Xiao, J.; Xie, Y.; Tang, R.; Luo, W. *Inorg. Chem*. **2003**, *42*, 107.
(30) Wang, J.; Grocholl, L.; Gillan, E. G. *Nano Lett*. **2002**, *2*, 899.
(31) Choi, J.; Gillan, E. G. *J. Mater. Chem*. **2006**, *16*, 3774.
(32) Choi, J.; Gillan, E. G. *Inorg. Chem*. **2005**, *44*, 7385.
(33) Grocholl, L.; Wang, J.; Gillan, E. G. *Chem. Mater*. **2001**, *13*, 4290.
(34) Desmoulins-Krawiec, S.; Aymonier, C.; Loppinet-Serani, A.; Weill, F.; Gorsse, S.; Etourneau, J.; Cansell, F. *J. Mater. Chem*. **2004**, *14*, 228.
(35) Choi, J.; Gillan, E. G. *J. Mater. Chem*. **2006**, *16*, 3774.
(36) Manz, A.; Birkner, A.; Kolbe, M.; Fischer, R. A. *Adv. Mater*. **2000**, *12*, 569.
(37) Sardar, K.; Rao, C. N. R. *Adv. Mater*. **2004**, *16*, 425.
(38) Sardar, K.; Dan, M.; Schwenzer, B.; Rao, C. N. R. *J. Mater. Chem*. **2005**, *15*, 2175.
(39) Sardar, K.; Deepak, F. L.; Govindaraj, A.; Seikh, M. M.; Rao, C. N. R. *Small* **2005**, *1*, 91.
(40) Vaidhyanathan, B.; Rao, K. J. *Chem. Mater*. **1997**, *9*, 1196.
(41) Sun, X. M.; Li, Y. D. *Angew. Chem., Int. Ed*. **2004**, *43*, 3827.
(42) Inumaru, K.; Baba, K.; Yamanaka, S. *Chem. Mater*. **2005**, *17*, 5935.
(43) Inumaru, K.; Koyama, K.; Miyaki, Y.; Tanaka, K.; Yamanaka, S. *Appl. Phys. Lett*. **2007**, *91*, 152501.
(44) Inumaru, K.; Koyama, K.; Imo-oka, N.; Yamanaka, S. *Phys. Rev. B* **2007**, *75*, 054416.
(45) Inumaru, K.; Nishikawa, T.; Nakamura, K.; Yamanaka, S. *Chem. Mater*. **2008**, *20*, 4756.
(46) Barry, S. T.; Richeson, D. S. *Chem. Mater*. **1994**, *6*, 2220.
(47) Kaskel, S.; Schlichte, K.; Chaplais, G.; Khanna, M. *J. Mater. Chem*. **2003**, *13*, 1496.
(48) Schwenzer, B.; Meier, C.; Masala, O.; Seshadri, R.; DenBaars, S. P.; Mishra, U. K. *J. Mater. Chem*. **2005**, *15*, 1891.
(49) Choi, D.; Blomgren, G. E.; Kumta, P. N. *Adv. Mater*. **2006**, *18*, 1178.
(50) Zhao, H. Z.; Lei, M.; Yang, X.; Jian, J. K.; Chen, X. L. *J. Am. Chem. Soc*. **2005**, *127*, 15722.
(51) Fischer, A.; Antonietti, M.; Thomas, A. *Adv. Mater*. **2007**, *19*, 264.
(52) Buha, J.; Djerdj, I.; Antonietti, M.; Niederberger, M. *Chem. Mater*. **2007**, *19*, 3499.
(53) Wiley, J. B.; Kaner, R. B. *Science* **1992**, *255*, 1093.
(54) Bonneau, P. R.; Jr, R. F. J.; Kaner, R. B. *Nature* **1991**, *349*, 510.
(55) Fitzmaurice, R. C.; Hector, A. L.; Parkin, I. P. *Polyhedron* **1993**, *12*, 1295.
(56) Fitzmaurice, R. C.; Hector, A. L.; Parkin, I. P. *J. Chem. Soc., Dalton Trans*. **1993**, 2435.
(57) Parkin, I. P. *Transition Metal Chem*. **2002**, *27*, 569.
(58) Parkin, I. P. *Chem. Soc. Rev*. **1996**, *25*, 199.
(59) Rao, L.; Kaner, R. B. *Inorg. Chem*. **1994**, *33*, 3210.
(60) Gillan, E. G.; Kaner, R. B. *Inorg. Chem*. **1994**, *33*, 5693.
(61) Gillan, E. G.; Kaner, R. B. *Chem. Mater*. **1996**, *8*, 333.
(62) Wallace, C. H.; Reynolds, T. K.; Kaner, R. B. *Chem. Mater*. **1999**, *11*, 2299.
(63) Cumberland, R. W.; Blair, R. G.; Wallace, C. H.; Reynolds, T. K.; Kaner, R. B. *J. Phys. Chem. B* **2001**, *105*, 11922.
(64) O'Loughlin, J. L.; Wallace, C. H.; Knox, M. S.; Kaner, R. B. *Inorg. Chem*. **2001**, *40*, 2240.
(65) Blair, R. G.; Anderson, A.; Kaner, R. B. *Chem. Mater*. **2005**, *17*, 2155.
(66) Song, B.; Jian, J. K.; Wang, G.; Lei, M.; Xu, Y. P.; Chen, X. L. *Chem. Mater*. **2007**, *19*, 1497.

purchased from Beijing Chemical Company, China. They were used without further purification.

Synthesis. In a typical run, crystalline boron powder was used as the precursor to react with Li_3N with a molar ratio of 3.5:1 (boron powder: Li_3N). Typically, 0.3243 g boron powders and 0.3 g Li_3N were mixed and ground together in an agate mortar. Then, the starting materials were pressed to a pellet and put into a stainless steel crucible as described in our previous report,[66] followed by placing the crucible into a silica ampule connected to an evacuating system. The silica ampule was evacuated to 3×10^{-5} Pa, then filled with 0.4 MPa high purity nitrogen (99.999%) and sealed. The silica ampule was heated to 850 °C in the conventional muffle and maintained for 4 h. Then, the power was shut off and the muffle was cooled down to room temperature naturally. In some cases, HNO_3 (95%) or HF (40%) was employed to treat the products. ***Caution!*** *HF and* HNO_3 *are extremely corrosive and very dangerous that can cause severe burns, and much attention should be paid in the manipulation process*. Similarly, 0.2314 g Al powder (99.99%) and 0.3 g Li_3N with a molar ratio of 3:1 (Al powder: Li_3N) were heated to 800 °C for 4 h to synthesize AlN. Then, 0.4 g Li_3N and 0.0833 g silicon powder were ground together and maintained at 850 °C for 4 h to obtain Si_3N_4 successfully. The reaction between Mo or Nb with Li_3N follow the similar route.

Characterization. X-ray powder diffraction (XRD) data were collected in reflection mode (Cu Kα radiation, $\lambda = 1.5418$ Å) on a Philips X'PERT MPD diffractometer using an etched glass plate sample holder and, for our samples, were operated at 40 kV and 40 mA. Lattice parameters were extracted from XRD data by the Rietveld method, using the program FULLPROF. The morphology of products were examined by a field emission scanning electron microscopy (FE-SEM, FEI XL 30 S-FEG), and semiquantitative composition analysis was performed by using an energy-dispersive spectroscope (EDX) attached to the FE-SEM with an Oxford energy-dispersive X-ray analysis system. To further investigate the morphological, size, and microstructure features of the as-prepared products, transmission electron microscopy (TEM) and high-resolution transmission electron microscopy (HRTEM) images of the samples were observed on a JEOL 2010 microscope with a high-brightness LaB_6 filament electron source at 120 and 200 kV, respectively. Samples were suspended in ethanol under ultrasonic vibration, and a few drops of the suspensions were brought onto a holey superthin carbon film on a copper grid for TEM observations.

III. Results and Discussion

BN is an important semiconductor material with the band gap of 6.1−6.4 eV for the cubic phase and has received much attention due to its potential applications in many fields ranging from abrasives and cutting tools to scratch-resistant coatings, etc. However, it is well-known that crystalline BN was very difficult to utilize except for a few cases. For instance, crystalline cubic boron nitride (*c*-BN), the second hardest material ($E = 45-50$ GPa), must be synthesized under extreme pressures (>5 GPa) and temperatures (>1500 °C), making it very expensive.[67] Industrial preparation of crystalline layered-form hexagonal boron nitrides (*h*-BN) was required to be performed at high temperature (>1450 °C), following a highly exothermic route of $3CaB_6 + B_2O_3 + 10N_2 \rightarrow 20BN + 3CaO$. Otherwise, amorphous BN will dominate the as-products. In this study, we show that by selecting an appropriate nitrogen source and boron source precursor, highly crystalline BN could be approached facilely at a moderate temperature by a simple reaction route. Here, crystalline boron powder (rhombohedral, ICDD-PDF: 31-0207) was selected as the boron source to react with Li_3N under nitrogen atmospheres at 850 °C for 4 h in a sealed crucible. Figure 1 shows an overview of the structural and morphological features of the as-products. One can see clearly that the XRD pattern before the treating process (Figure 1a, top) was composed of four crystalline phases, that is, Li_3BN_2 (ICDD-PDF: 13-0393), hexagonal Li_3N (ICDD-PDF: 65-1896), rhombohedral BN (ICDD-PDF: 45-1171), and hexagonal BN (ICDD-PDF: 34-0421). XRD patterns for the products after the washing process with 95% HNO_3 (Figure 1a, bottom) can be indexed well with the hexagonal BN (space group *P*63/*mmc*) and rhombohedral BN (space group *R*3*m*) as indicated by vertical lines, and no other diffraction peaks from impurities were detected under the X-ray diffractometer's resolution (X'PERT MPD), suggesting that Li_3BN_2 could be eliminated completely by the treating process only with the formation of two types of X-ray purity phases BN.

Sharp diffraction peaks indicated the highly crystalline BN were obtained. The cell lattice is calculated to be $a_1 = 0.25061$ nm, $c_1 = 0.66813$ nm for hexagonal BN phase and $a_2 = 0.2505$ nm, $c_2 = 1.011$ nm for rhombohedral BN phase, which are in good agreement with standard ICDD-PDF cards. The TEM image (Figure 1b) shows that the treated BN products have a layer-shaped structure. The HRTEM image (Figure 1c, corresponding to the marked area as shown in Figure 1b) displays the well-developed and distinct lattice image, suggesting that highly crystalline BN products were approached. The interplanar spacing of 0.2013 and 0.2099 nm can be assigned to d_{100} and d_{101} values of hexagonal BN (ICDD-PDF: 34-0421), respectively. The inset of Figure 1c shows the selected area electron diffraction (SAED) pattern. Typical Debye−Scherrer diffraction dots revealed the single-crystal nature of the obtained products and can be easily indexed to the characteristic phase of hexagonal BN. Figure 1d and e show the selected area fast Fourier transform (FFT) images corresponding to the randomly selected spots as shown in Figure 1c, which further confirm the intrinsic hexagonal as well as the single-crystal nature of the obtained BN products. The energy dispersive X-ray analysis (EDX) pattern (Figure 1f) shows that only B, N, C, and O elements were detected in the treated BN sample Here, no organic nitrifying reagent was involved, and the amorphous carbon as a common contamination in carbothermal reduction or gas phase/solid-state precursor decomposition route was thus prevented in this route from the source. It is thus speculated that the carbon signal may originate from the carbon-coated copper grid used for the TEM observation and the trace O element originates from the O_2 and H_2O absorbed on the sample during the treating process. It should be noted that when using B_2O_3 as the B source to react with Li_3N, only the amorphous BN can be approached as reported in ref 66, revealing the advantage of using the B element as a precursor to synthesize crystalline BN. However, crystalline BN was obtained by this facile route, suggesting the powerful nitrification ability of Li_3N.

To further test the feasibility and effectiveness of the route between a single-substance element and Li_3N, we show another case of the synthesis of aluminum nitrides (AlN). AlN is an important III−V nitride semiconductor with the wide band gap of 6.2 eV. The conventional conversion from Al or Al_2O_3 to AlN was often required to be performed at

(67) Chung, H. Y.; Weinberger, M. B.; Levine, J. B.; Kavner, A.; Yang, J. M.; Tolbert, S. H.; Kaner, R. B. *Science* **2007**, *316*, 436.

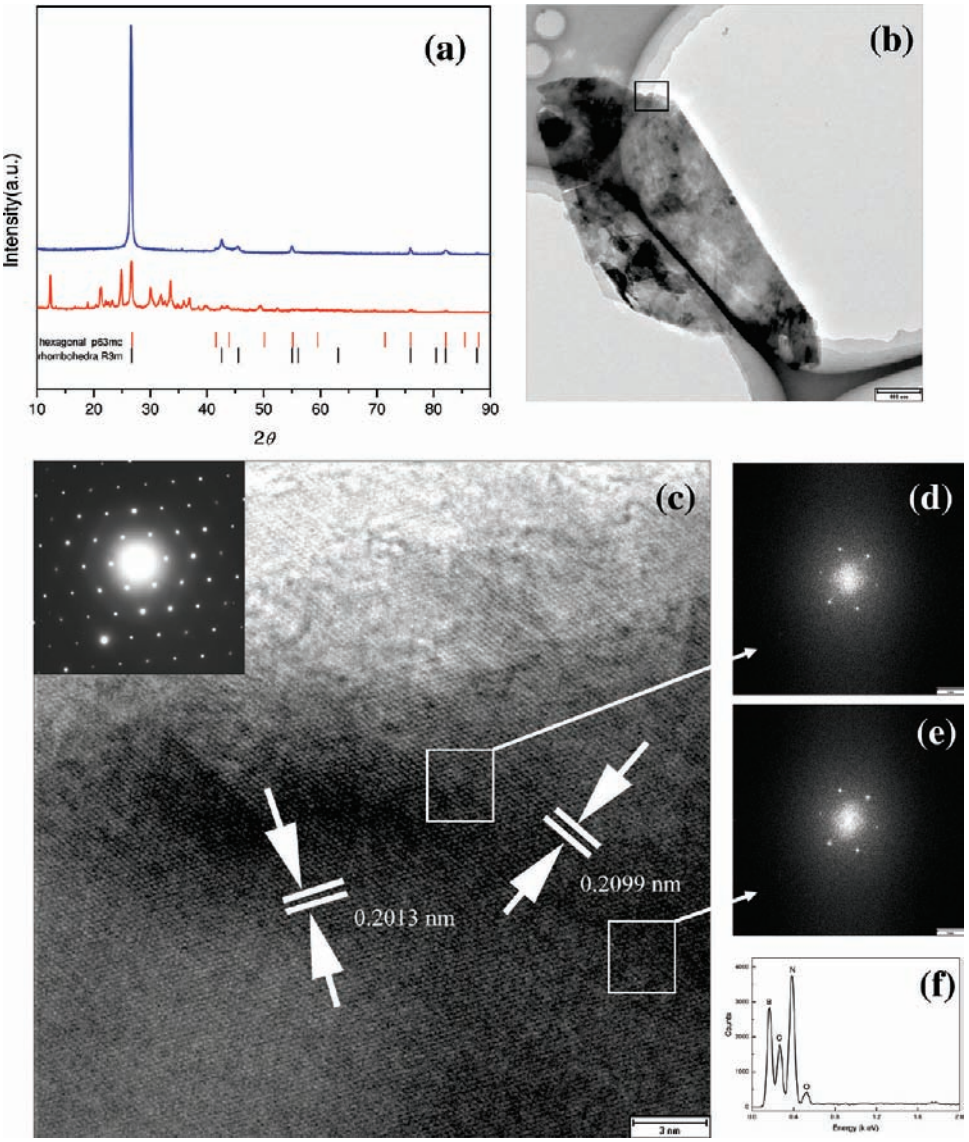

Figure 1. (a) XRD pattern for the products before (bottom curve) and after (top curve) treating from the reaction between Li_3N and boron. Vertical bars (|) indicate the positions of Bragg peaks for standard rhombohedral BN (ICDD-PDF: 45-1171) and hexagonal BN (ICDD-PDF: 34-0421), respectively. (b) TEM image of the treated BN. (c) HRTEM image corresponding to the selected areas as marked in part b. (d and e) FFT images corresponding to the randomly selected spots shown in part c. (f) EDX pattern of the treated products.

high temperature (> 1300 °C) under a NH_3 atmosphere or carbothermal reduction at 1200 °C. Figure 2a shows the XRD pattern of the products obtained from the reaction between Li_3N and Al element before and after the washing process. The XRD pattern (Figure 2a, top) indicates distinctly that the as-prepared products were composed of two phases: AlN (hexagonal, ICDD-PDF: 65-3409) and Li_3AlN_2 (cubic, ICDD-PDF: 65-3189) as indicated by arrows. The XRD pattern (Figure 2a, bottom) for the treated products can be indexed well with hexagonal AlN, and no other peaks from impurity phases were detected. The TEM overview image (Figure 2b) displays the irregular morphological features of the treated AlN samples. Similar irregular morphology features have also been observed in AlN obtained from the reaction between α-Al_2O_3 and Li_3N.[66] The crystallinity of the obtained AlN in this study was further confirmed by HRTEM investigations. The HRTEM micrograph (Figure 2c) shows the highly crystalline features of the as-obtained AlN while the corresponding SAED pattern (top-left inset in Figure 2c) is indexed well to the reflections of hexagonal AlN (ICDD-PDF: 65-3409), providing further evidence for the formation of AlN. The characteristic diffraction dots in the SAED pattern and FFT image (bottom-left inset in Figure 2c) undoubtedly suggest the single-crystal nature of as-prepared AlN.

$$Li_3N + Ga \rightarrow Li_3GaN_2 + Li \quad (1)$$

$$Li_3GaN_2 + Ga \rightarrow GaN + Li \quad (2)$$

$$Li_3N + Ga \rightarrow GaN + 3Li \quad (3)$$

These two representative cases show the effective nitrifying ability of this facile MSSM route in converting a single substance into crystalline nitrides. Here, Li_3N displays a more powerful nitrifying ability over these previously used nitrifying reagents such as g-C_3N_4 or melamine.[50,68] It has

(68) Zhao, H. Z.; Lei, M.; Chen, X. L.; Tang, W. H. *J. Mater. Chem.* **2006**, *16*, 4407.

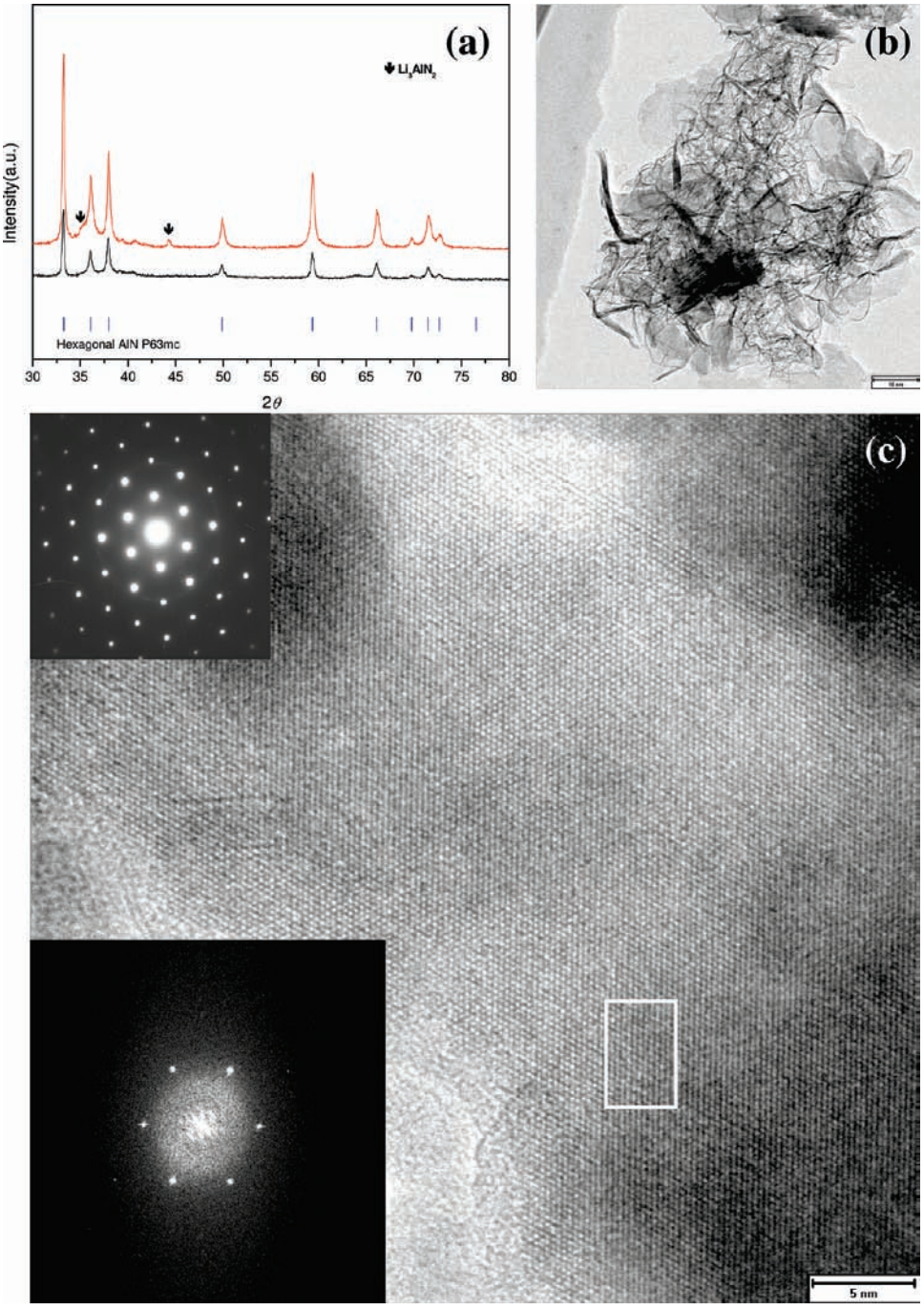

Figure 2. (a) XRD pattern for the products before (top curve) and after (bottom curve) treating from the reaction between Li_3N and Al. Vertical bars (|) indicate the positions of Bragg peaks for standard hexagonal AlN (ICDD-PDF: 65-3409). (b) TEM overview image of the treated AlN. (c) HRTEM image of the as-treated AlN. The up-left inset is the SAED pattern, and the bottom-left inset presents the FFT image corresponding to the marked area shown in part c.

been verified that Li_3N reacts with Ga to form Li_3GaN_2 (eq 1); then, the as-prepared Li_3GaN_2 continues to react with Ga to produce GaN (eq 2), and the overall reaction mechanism can be described by eq 3.[69−71]

Being inspired by the two-step reaction mechanism for GaN, it is speculated that the fabrication of the other IIIA nitrides such as BN and AlN also follow the similar two-step formation process which may serve as the intrinsic mechanism for the reaction between a IIIA group element and Li_3N since the similar products of XN and Li_3XN_2 (X = B, Al) were obtained together in the synthesis of BN and AlN, as in the grown GaN single crystal by the Li_3N flux method.[69,70] The precursors of B powder, Al powder, and nitrifying reagents of Li_3N are in solid state prior to reaction. The latter will discompose into active Li and N atoms/ions upon heating at elevated temperatures. Then, the B or Al element is nitrified by N and Li atoms/ions to form ternary nitrides of $Li_xB_yN_z$ or $Li_xAl_yN_z$ which further reacts with B or Al atoms, and then, crystalline BN or AlN present itself from the

(69) Wang, G.; Jian, J. K.; Song, B.; Chen, X. L.; Wang, W. J.; Song, Y. T. *Appl. Phys. A: Mater. Sci. Process.* **2006**, *85*, 169.
(70) Song, Y. T.; Wang, W. J.; Yuan, W. X.; Wu, X.; Chen, X. L. *J. Cryst. Growth* **2003**, *247*, 275.
(71) Chen, X. L. *Sci. Technol. Adv. Mater.* **2005**, *6*, 766.

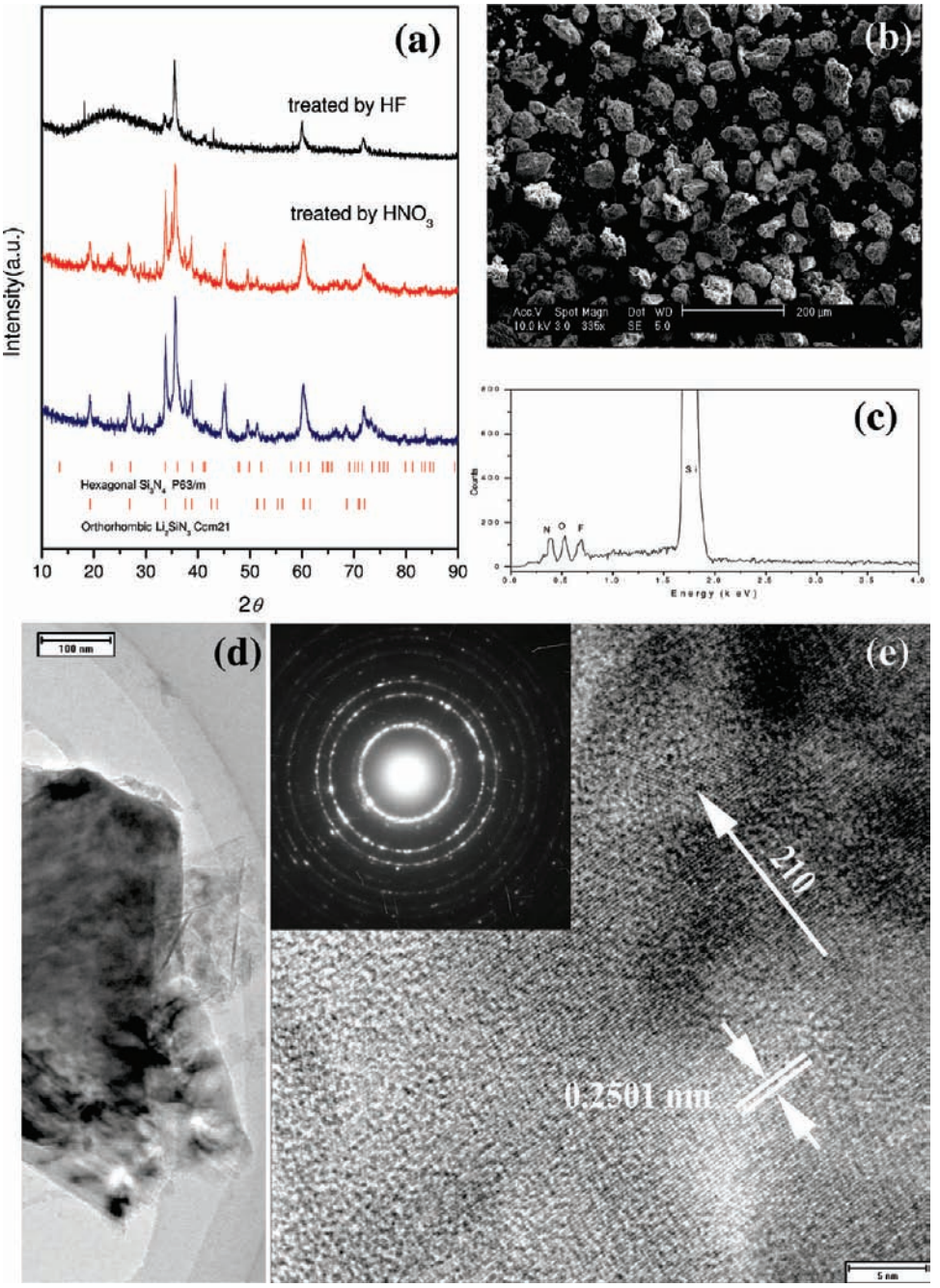

Figure 3. (a) XRD pattern for the products before treatment (bottom curve), after treatment with HNO_3 (middle curve), and after treatment with HF (top curve) from the reaction between Li_3N and Si. Vertical bars (|) indicate the positions of Bragg peaks for standard orthorhombic $LiSi_2N_3$ (ICDD-PDF: 26-1186) and hexagonal Si_3N_4 (ICDD-PDF: 33-1160), respectively. (b) SEM image of the products treated by HF. (c) EDX pattern of the products after treatment with HF. (d) TEM image of the products after treatment with HF. (e) HRTEM image of the products. The inset is the corresponding SAED pattern.

saturated Li−X−N ternary system. Here, the formation of intermediate products Li_3XN_2 serves as the key role to drive the reaction. In fact, the initial molar ratio of Li_3N to X (X = B, Al) chooses the final products in the form of binary or ternary nitrides, i.e., according to the Li−N−X (X = B, Al) ternary phase diagram, the desired nitride is the Li_3XN_2 phase or the coexistence of XN and Li_3XN_2 can be approached by designing the ratio of starting materials before the route is ignited. Although the two-step reaction mechanism for BN and AlN is not as well-evidenced as that for GaN, the products obtained with different processes can still demonstrate the validity of this mechanism.

Further, it is found that this two-step reaction mechanism can also be applied to describe the reaction mechanism between Li_3N and other single-substance elements than only the IIIA group element, such as the IVA element of silicon. α-Si_3N_4, for instance, was normally prepared at more than 1350 °C using Si powder and N_2 as the precursors while β-Si_3N_4 was required to be synthesized at more than 1500 °C for 72 h using Si powder and NH_3 as precursors. Recently, Chen et al. reported the reaction between Si and Li_3N with a variation ratio from 2:4.5 to 4:4.5.[72] It was found that a large

(72) Song, B.; Jian, J. K.; Cai, G. M.; Lei, M; Bao, H. Q.; Li, H.; Xu, Y. P.; Wang, W. Y.; Han, J. C.; Chen, X. L. *Solid State Ion.* **2009**, *180*, 29.

series of molar ratios (Li_3N to Si) can only approach the ternary nitride of Li_2SiN_2, and then, it is speculated that for the case of Si, there also exist a two-step reaction process as described by eq 4. Here, we try to increase the molar ratio of Si to Li_3N to facilitate eq 4 to proceed.

$$Si + Li_2SiN_2 \rightarrow Si_3N_4 + Li \quad (4)$$

Figure 3a shows the XRD patterns of the products before and after the treating process. One can see clearly that the unvarnished products were composed of $LiSi_2N_3$ (ICDD-PDF: 26-1186) and hexagonal Si_3N_4 (ICDD-PDF: 33-1160) [bottom XRD pattern in Figure 3a]. After treatment with HNO_3 (95%), the XRD pattern (middle XRD pattern in Figure 3a) shows no obvious change appearing in the curves, indicating the highly chemical stability of the products. In order to eliminate the $LiSi_2N_3$ phase, the more rigorous acid washing process was involved by using HF(40%), and then, only the Si_3N_4 phase can be detected (top XRD pattern in Figure 3a). Figure 3b shows the representative field-emission scanning electron microscopy (FESEM) image of the treated Si_3N_4 samples by HF, and irregular morphologies are observed from this panoramic view. The EDX pattern (Figure 3c) shows the element composition of the treated products agreeing well with silicon nitrides while the trace O and F impurities can be ascribed to the contamination in the treating process. The TEM image (Figure 3d) further displays the morphological features of the treated Si_3N_4. The HRTEM image (Figure 3e) shows the clear stripe image. The lattice spacing is 0.2501 nm for the (210) plane, which agrees well with the standard ICDD-PDF card, 33-1160, for Si_3N_4 with d_{210} = 0.2489 nm. The corresponding ringlike SAED pattern (inset in Figure 3e) indicates that the microstructures of the as-prepared Si_3N_4 are polycrystalline and the diffraction rings can be easily assigned to the characteristic reflections of hexagonal Si_3N_4, confirming the previous XRD and HRTEM results. Here, hexagonal Si_3N_4 were obtained successfully like BN and AlN, suggesting that the two-step process may be the general mechanism between Li_3N and a single substance. In comparison with the synthesis of BN and AlN, Li_2SiN_3 and then Li_2SiN_2 serve as the intermediate compounds and then, for the case of Si_3N_4, the two-step equation can be depicted by eqs 5 and 6, respectively; eq 7 denotes the general reaction mechanism.

$$Li_3N + Si \rightarrow LiSi_2N_3 + Li \quad (5)$$

$$LiSi_2N_3 + Si \rightarrow Si_3N_4 + Li \quad (6)$$

$$4Li_3N + 3Si \rightarrow Si_3N_4 + 12Li \quad (7)$$

From the viewpoint of enthalpy, the heat of formation of the binary Si_3N_4 (ΔH_f = −651.83 kJ·mol^{-1} at 1000 K) is lower than that of the Li_3N (ΔH_f = −120.46 kJ·mol^{-1} at 1000 K) and provides the driving force for the MSSM route. The thermodynamic calculation of enthalpies (ΔH_{rxn}) for eq 7 is −171 kJ·mol^{-1} at 1000 K and 44.85 kJ·mol^{-1} at 298 K which is the reason why the reaction between Li_3N and Si should be heated to high temperature. To further probe the detailed reaction mechanism, the in situ characterization means was required, such as the differential thermal analysis (DTA), etc. However, the flat-bottomed Al_2O_3 ceramic crucible used for the DTA measurement will be eroded by the Li_3N as reported in ref 66, and it is very difficult to record the reaction parameter including exothermic or endothermic processes in real time. In addition, the MSSM reactions between Li_3N and single elements need a sealed system to realize two aims: (1) maintain a stable N_2 pressure to prevent the decomposition of the Li_3N at low temperature; (2) prevent the spreading of the active debris such as Li^+ and N^{3-} from the decomposition of Li_3N, that is, transforming most precursors into nitrides. As mentioned above, however, the DTA measurement could reveal the detailed reaction mechanism in real time; the flowing N_2 will destroy this quasi-equilibrium environment and failed to approach the desired nitrides as reported in ref 66. So, it is unreasonable to probe the detailed reaction mechanism of the MSSM route by using conventional characterizations means such as DTA, etc. Although the detailed reaction mechanism cannot be well-unveiled, the general reaction mechanism can still be summarized by investigating the product composition with different molar ratios and reaction periods.

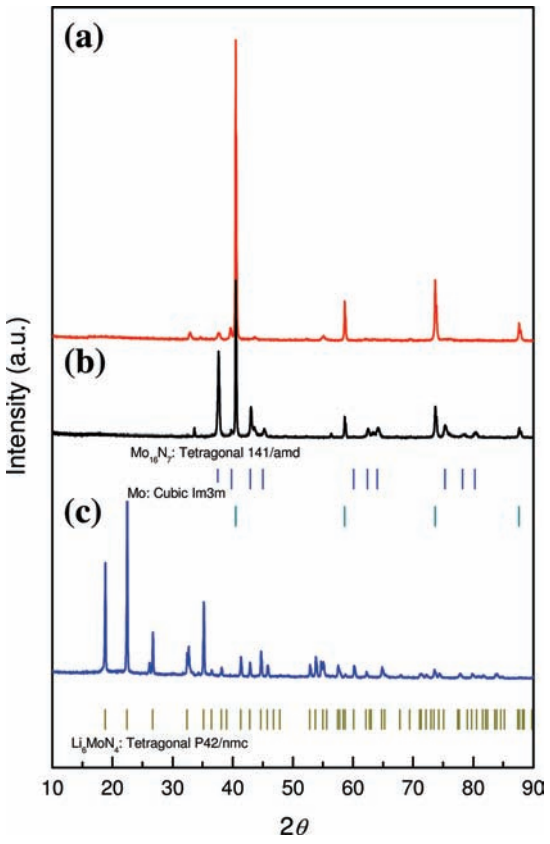

Figure 4. XRD pattern for the products from the reaction between Mo and Li_3N with ratios of (a) 2:1 (Mo to Li_3N) and (b) 4:1 (Mo to Li_3N). Vertical bars (|) indicate the positions of Bragg peaks for standard Mo (ICDD-PDF: 42-1120) and $Mo_{16}N_7$ (ICDD-PDF: 23-1256), respectively. (c) XRD pattern for the products from the reaction between Mo and Li_3N with a ratio of 1:5 (Mo to Li_3N). Vertical bars (|) indicate the positions of Bragg peaks for standard card of Li_6MoN_4 (ICDD-PDF: 65-1202).

Furthermore, eq 6 reveals another striking feature for this pathway that this route can also be applied to synthesize multinitrides. Usually, mononitrides must be prepared at high temperatures and high pressures. Cubic NbN, for instance, is normally approached at more than 1600 °C under the N_2 atmosphere of 16 MPa, as are TaN and CrN. Multinitrides such as Ta_2N, Ta_3N_5, Nb_4N_3, Nb_2N, and Cr_2N will

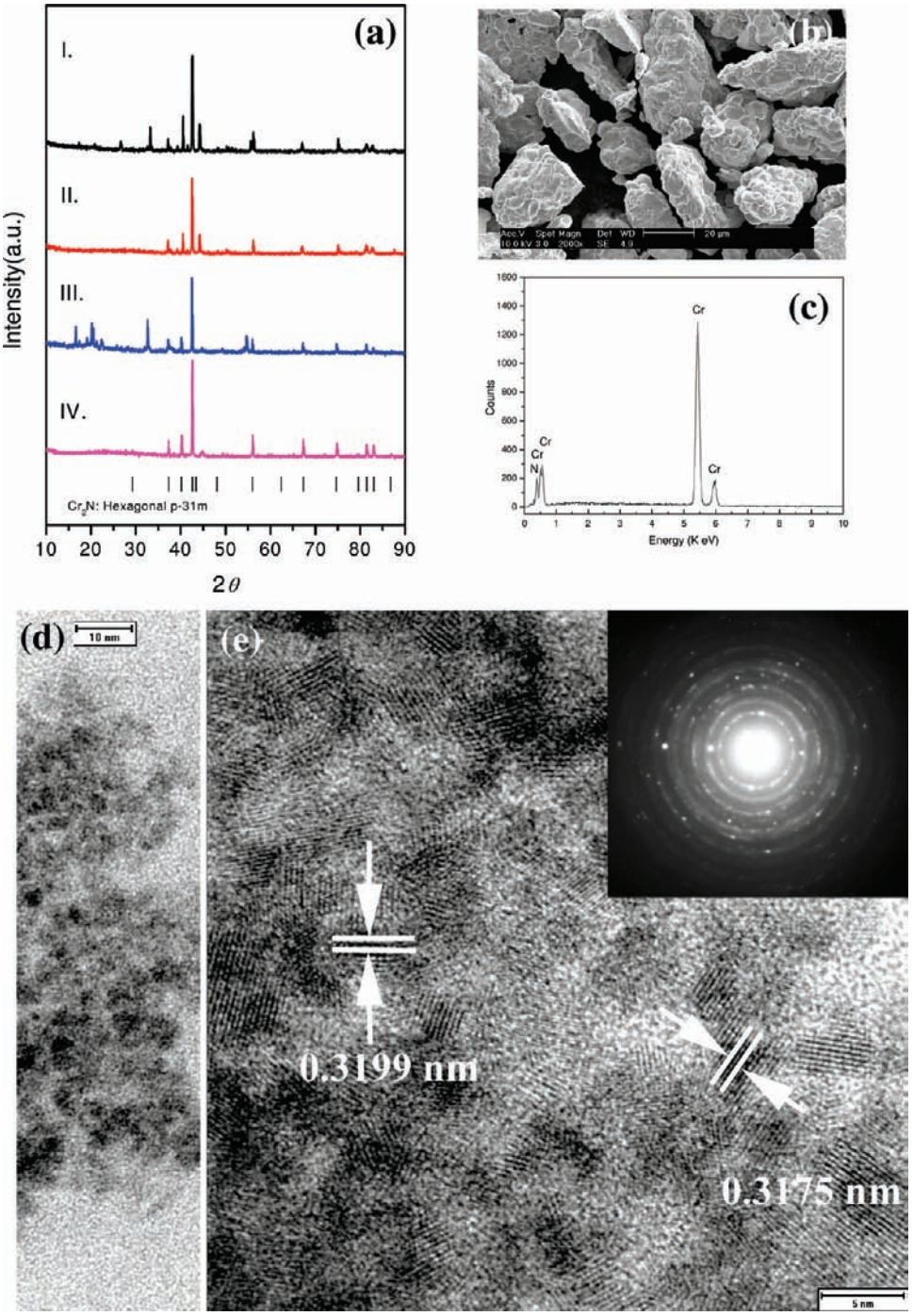

Figure 5. (a: I and II) XRD pattern of products before and after treating by DI water from the reaction of Cr to Li_3N with the molar ratio of 1:1. (III and IV) XRD pattern of the products before and after treating by DI water from the reaction of Cr to Li_3N with the molar ratio of 2:1 (Cr to Li_3N). Vertical bars (|) indicate the positions of Bragg peaks for the standard card of Cr_2N (ICDD-PDF: 35-0803, hexagonal, $\bar{P}31m$). (b) SEM image of the treated products. (c) EDX pattern of the treated products. (d) TEM image of the treated products. (e) HRTEM of the treated products; (inset) SAED pattern.

otherwise dominate the products.[56,64] Similar situations are also true for the reaction between Li_3N and single substances. For some elements, only multinitrides, such as $Mo_{16}N_7$, Cr_2N, or Ta_4N_5, etc. can be approached by this route. Figure 4 shows the XRD pattern of the untreated products from the reaction of Mo and Li_3N with a ratio (Mo to Li_3N) of 2:1 (Figure 4a), 4:1 (Figure 4b), and 1:5 (Figure 4c) at 850 °C for 4 h. Phase identifications indicated that the products in Figure 4a are remnants Mo (ICDD-PDF: 42-1120) and $Mo_{16}N_7$ (ICDD-PDF: 23-1256), respectively. Figure 4b shows that the $Mo_{16}N_7$ phase gradually dominated. As the molar ratio is increased to 1:5, only the ternary nitrides of Li_6MoN_4 (ICDD-PDF: 65-1202) were obtained without any trace of impurity phase under the instrument's resolution (Figure 4c). By a similar process, we synthesized Cr_2N at 850 °C, with the molar ratio of 1:1 and 2:1 for Cr to Li_3N, respectively. Figure 5a(I) and (II) shows the XRD pattern of the products before and after treating with the molar ratio of 1:1 (Cr to Li_3N), respectively. One can see clearly that, by a simple washing process with deionized (DI) water, the X-ray purity phase of Cr_2N (ICDD-PDF: 35-0803, hexagonal, $\bar{P}31m$) was approached, and similar results for the reaction

with a molar ratio of 2:1 (Cr to Li_3N) were shown in Figure 5a (III) [unwashed] and (IV) [washed], respectively. Figure 5b presents the overview morphological features of washed Cr_2N from the reaction with molar ratio of 1:1 (Cr to Li_3N). Only Cr and N elements were detected in EDX analysis (Figure 5c). The TEM image (Figure 5d) shows that the treated Cr_2N are composed of particles with varied sizes and irregular shapes. The HRTEM image (Figure 5e) clearly indicates the plane spacing being 0.3199 and 0.3175 nm, taken on different particles, which corresponds well to the (101) lattice planes of hexagonal Cr_2N with $d_{101} = 0.3252$ nm. The SAED pattern (Figure 5e, inset) shows the typical Debye−Scherrer diffraction rings for the polycrystalline. These rings can be facilely assigned to the characteristic reflections of hexagonal Cr_2N (ICDD-PDF: 35-0803, hexagonal, $\bar{P}31m$). In this route, the high molar ratio of Cr to Li_3N (>4:1) will lead to the formation of ternary nitrides Li_9CrN_5 (ICDD-PDF: 36-0695).

$$Li_3N + X \rightarrow LiX_AN_B + Li \quad (8)$$

$$LiX_AN_B + X \rightarrow X_CN_D + Li \quad (9)$$

On the basis of available results, we propose a general two-step reaction to depict the mechanism between Li_3N and a single element as shown in eqs 8 and 9. As mentioned previously, the molar ratio of Li_3N to the single element serves as the key to determining the detailed reaction process. If the molar ratio of Li_3N to the element is located in the Li-rich area, the products are mainly composed of ternary nitrides LiX_AN_B. This means that only eq 8 occurs: If the molar ratio is located in the element-rich area, the products are often found to be the mixture of LiX_AN_B and X_CN_D, indicating that eq 9 also occurred following eq 8 taking place as a two-step process. Equation 9 determines the products to present in the form of mono- or multinitrides.

We have reported that the reaction between Li_3N and oxides, for example, Cr_2O_3, was also a two-step process as depicted by eqs 10 and 11.[66] First, the active lithium atoms, originating from the partial decomposition of Li_3N, reduce Cr_2O_3 to the active Cr atoms/ions (eq 10). Then, the produced Cr atoms/ions are nitrified by active nitrogen atoms/ions or Li_3N directly to form cubic CrN (eq 11). From the viewpoint of element conservation, the as-prepared Cr_2N in this study requires another N to form Cr_2N_2 (CrN) [eq 12], and this transformation from Cr_2N (low-temperature phase) to CrN (high-temperature phase) can only be realized with the assistance of a powerful driving force. In contrast with eq 11, it is speculated that the fact that the effort failed to approach CrN could be ascribed to the weak driving force involved in eq 9. The formation of CrN and thermodynamically favored byproducts of Li_2O both serve as the driving force to overcome the energy barrier in eq 11, especially the latter: great heat was released during the formation of Li_2O that plays the key role in pushing the reaction while only the formation of Cr_2N serves as the driving force. Then, the multinitrides were found to dominate the products. Similar cases are also encountered in the synthesis of NbN, TiN, ZrN, etc. by the MSSM route.

$$Li_3N + Cr_2O_3 \rightarrow Cr/Cr^{3+} + N^{3-} + Li_2O \quad (10)$$

$$Cr/Cr^{3+} + N/N^{3-}(Li_3N) \rightarrow CrN \quad (11)$$

$$Li_3N + Cr_2N \rightarrow CrN + Li \quad (12)$$

Due to the lack of thermodynamic data for these multinitrides as produced, we cannot calculate the precise theoretical energy released in the reactions, as well as the actual reaction temperatures, etc. However, this route has successfully approached many types of nitrides including crystalline BN, AlN, multinitrides of Si_3N_4, Cr_2N, and Mo_2N, etc., suggesting the effective nitrified ability of Li_3N in conversion processes from single substances to nitrides. It should be noted that, although O and F impurities were involved in the washing process, the content is much less compared with the contaminations in conventional carbothermal reduction or using oxides as the precursors. Further, this study reveals a general principle for selecting precursors to synthesize nitrides using Li_3N that the precursor should provide effective anions such as O^{2-}, S^{2-}, Cl^{1-}, Br^{1-}, etc to combine with Li^+ to form thermodynamically favored Li_2O, LiCl, or LiBr. In this process, the great heat acts as the driving force and push the N^{3-} to unite with cation to form nitrides, this is also the typical SSM route reaction mechanisms.

IV. Conclusions

In this study, we present a detailed investigation on the MSSM route to transform single substances to nitrides using Li_3N as the nitrifying reagent. The possible two-step reaction mechanism was proposed. The fascination of this pathway is the diversity of products, not only binary nitrides (mononitrides, multinitrides) but also ternary nitrides can be approached, providing a promising route to meet the increasing demand for materials synthesis in energy saving and environmental protection.

Acknowledgment. This work is supported financially by the National Natural Science Foundation of China (grant No. 50902037), Ludo Frevel Crystallography Scholarship Award for B.S. (The International Centre for Diffraction Data, ICDD, USA), China Postdoctoral Science Foundation funded project (20090451008), Development Program for Outstanding Young Teachers in Harbin Institute of Technology (HIT), HITQNJS.2009.065., and the Chinese Academy of Sciences.